ELSEVIER

Polymer 40 (1999) 4143–4147

polymer

Polymer Communication

The influence of activation on the solution state of cellulose dissolved in *N*-methylmorpholine-*N*-oxide-monohydrate

Thomas Röder, Bernd Morgenstern*

Technische Universität Dresden, Institut für Physikalische Chemie und Elektrochemie, 01062 Dresden, Germany

Received 1 June 1998; received in revised form 18 September 1998; accepted 18 September 1998

Abstract

The solution state of cellulose dissolved in *N*-methylmorpholine-*N*-oxide-monohydrate (NMMNO·MH) was investigated by static laser-light scattering. Special emphasis was placed on the potential influence of activation procedures. The light-scattering measurements were analysed in terms of Guinier–Zimm plots. Molecular masses of the order of several million g mol^{-1} were observed. This indicates that cellulose aggregates exist and that the aggregates comprise several hundred cellulose chains. The radii of gyration of these aggregates exceed 160 nm. The overall scattering functions can be separated into two partial scattering contributions. This reflects a bimodal distribution of the particulate phase, consisting of large and small aggregates. Activation of cellulose prior to dissolution leads to particles consisting of significantly fewer cellulose molecules than without activation. However, the size of the aggregates does not change significantly.

Keywords: Cellulose; *N*-methylmorpholine-*N*-oxide; Activation

1. Introduction

The monohydrate of *N*-methylmorpholine-*N*-oxide (NMMNO·MH) is a solvent for cellulose [1,2] that does not form a cellulose derivative [3]. In the last few years it has gained increasing importance for the production of a new class of man-made cellulose fibres [4–6], the so-called LYOCELL fibres [7]. The properties of LYOCELL fibres include high tenacity as well as high fibrillation tendency. These properties are due to a high degree of crystallinity and a high orientation of the cellulose chains in the non-crystalline regions of the fibres [8]. For the preparation of spinning solutions [6], shredded pulp is dispersed in an aqueous solution of NMMNO containing 40–50% water for about 1 h. Afterwards water is removed under vacuum at elevated temperatures. The cellulose dissolves, giving the appearance of a clear solution when the water content reaches 15 to 13%. An additional pretreatment of the cellulose is not necessary.

In contrast to NMMNO·MH, dissolution of cellulose usually cannot be carried out in one step, since the highly ordered structure of native cellulose prevents the access of solvent molecules. Therefore, prior to dissolution, in an activation process the crystalline domains of cellulose have to be transformed into disordered regions. The hydrogen-bond system of cellullose is disintegrated simultaneously to some extent. These structural alterations improve the accessibility of cellulose chains for the attack of solvent molecules [9], a prerequisite for the dissolution of native cellulose.

Activation can be carried out by swelling of cellulose in a highly polar medium or by thermomechanical treatments [10,11]. The activation process may not completely disintegrate the ordered domains of cellulose. It is likely that cellulose is not molecularly dispersed in solutions but is organized in more or less extended aggregates of still ordered cellulose molecules [12,13]. Activation may even influence the solution state of cellulose when dissolved in NMMNO·MH. Light scattering was used to obtain useful insight into the nature of the structures existing in cellulose solutions. We report the results of static light-scattering measurements carried out on solutions of two cellulose materials that were activated by different methods.

2. Experimental

2.1. Materials

N-Methylmorpholine-*N*-oxide-monohydrate (NMMNO·MH) was reagent grade (Merck) and had a melting point

* Corresponding author. Tel.: +49-351-463-4609; fax: +49-351-463-7164.
E-mail address: bernd.morgenstern@chemie.tu-dresden.de (B. Morgenstern)

0032-3861/99/$ - see front matter
PII: S0032-3861(98)00674-0

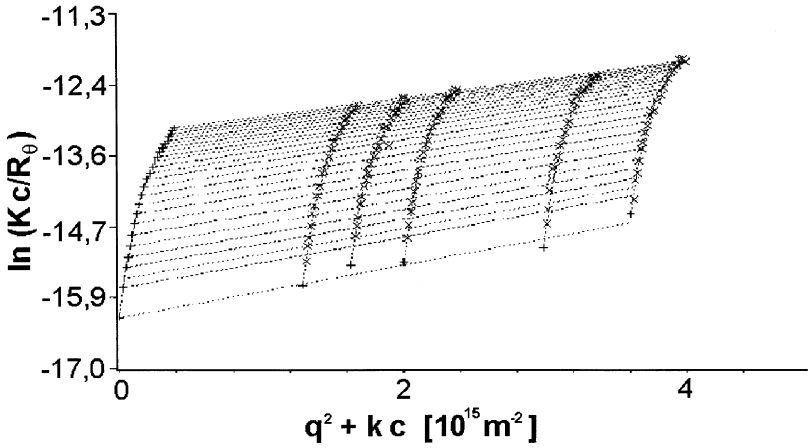

Fig. 1. Guinier–Zimm plot of sample V60A dissolved in NMMNO·MH at 80°C.

of 72–73°C. The cellulose materials used in this study were Heweten-201® (H201), a powdered cotton linters degraded by acid hydrolysis, and a coniferous sulfate pulp, Buckeye V60 (V60). V60 was shredded by a pin mill. The initial samples had a degree of polymerization (DP) of 175 (H201) and 535 (V60), respectively. The DPs were estimated by intrinsic viscosity measurements in cuoxam [14].

2.2. Cellulose activation

Cellulose was activated by three different procedures:

1. 10 g of cellulose (H201 and V60, respectively) were slurried in 500 cm^3 of deionized water overnight, filtered through a glass frit and pressed out. The remaining water content was 39.2% for H201 and 36.7% for V60.
2. 20 g of cellulose (H201) was suspended in 500 cm^3 of NaOH solution (20 wt%) and swollen overnight at 4°C. Afterwards, the cellulose was carefully rinsed with deionized water until neutralization and pressed out. The remaining water content was 40.3%.
3. V60 cellulose was immersed in liquid ammonia for a few minutes. Then the ammonia was removed by a steam explosion process [15]. This procedure results in a highly disintegrated and dry material.

2.3. Preparation of cellulose solutions

For the purpose of purification, approximately 15 g of molten NMMNO·MH was filtered through a heated glass frit (pore size 1.6 μm) at 90°C into a 50 cm^3 three-necked flask. The NMMNO·MH was weighed after cooling. Then, the calculated amount of cellulose sample was added to the re-molten NMMNO·MH under nitrogen and stirring with a magnetic stirrer. The cellulose was dissolved during 4 to 30 h. Dissolution of the non-activated samples required the longer periods of time. Completion of cellulose dissolution was assumed to have occurred when solid or swollen cellulose particles were no longer visible. Once dissolution was complete the solutions were stirred for a further 2 h. The cellulose solutions were filtered through a heated glass frit of 16 μm pore size into dustless 10 cm^3 ampoules with the aid of a light vacuum of 250 mbar. Excess water was removed after 10–15 min. The ampoules were then sealed. The solutions had cellulose concentrations in the range from 0.2% to 3%. No antioxidant was added since tests with n-propyl gallate [16] resulted in intensive discoloration that would have interfered with the light-scattering measurements.

2.4. Static laser-light-scattering measurements

A SLS-2 goniometer (SLS Systemtechnik, Germany) with a He–Ne laser ($\lambda = 632.6$ nm) as light source was used. The light beam was vertically polarized with respect to the scattering plane. The device is equipped with an external heating unit that controls the temperature in the 0–150°C range with an accuracy of ±1°C. The scattering measurements were carried out in the angular range 30–145° with an intercept length of 5°. All measured data were corrected with respect to self-absorption since the cellulose solutions were slightly brown in colour. Corrected quantities, $(K_c/R_\theta)_{corr}$, were calculated from Eq. (1):

$$\left(\frac{Kc}{R_\theta}\right)_{corr} = Kc\left(\frac{R_{\theta_C}}{T_C} - \frac{R_{\theta_{MMO}}}{T_{MMO}}\right)^{-1} \quad (1)$$

The quantities K, c and R_θ are explained in Appendix A. T_C and T_{MMO} denote the transmissions of the cellulose solution and the solvent, respectively. They follow from

$$\log T = -E \quad (2)$$

where E is the extinction measured with a Shimadzu UV-2101PC spectrometer at 632.8 nm.

The refractive index of NMMNO·MH at 80°C is $n_0 = 1.4638$ and was determined with an Atago RX-5000 digital refractometer. The refractive index increment of cellulose in NMMNO·MH was estimated by Seger [17] to be $\delta n/\delta c = 0.068$ cm^3 g^{-1} at 85°C. The value for $\delta n/\delta c$ was measured with a DR-1 differential refractometer (SLS Systemtechnik,

Table 1
Results of static light-scattering measurements on initial and activated cellulose samples dissolved in NMMNO·MH

Sample	Swelling medium	DP_{cuoxam}	M_w (g mol^{-1})	n_w [a]	R_g (nm)	A_2 (mol cm^3 g^{-2})	D (g l^{-1})
H201	—	175	18.9×10^6	665	188	3.9×10^{-6}	1.1
H201W	Water	175[b]	9.0×10^6	320	192	1.9×10^{-6}	0.5
H201S	20% NaOH	175[b]	5.2×10^6	180	177	3.7×10^{-6}	0.4
V60	—	535	55.2×10^6	635	204	2.1×10^{-6}	2.6
V60W	Water	510	17.5×10^6	210	171	1.9×10^{-6}	1.4
V60A	Liquid ammonia	485	10.7×10^6	135	167	4.0×10^{-6}	0.9

[a] $n_w = M_w/(162DP_{cuoxam})$.
[b] The DP was not determined, and the value of the unactivated sample was taken.

Germany), equipped with a He–Ne laser at 632.8 nm. For sample V60A, $\delta n/\delta c$ was found to be (0.061 ± 0.007) cm^3 g^{-1} at 80°C. This value was used for all cellulose samples.

3. Results and discussion

The results of the light-scattering measurements were evaluated successfully in terms of Guinier–Zimm plots (see Appendix A). As an example, the Guinier–Zimm plot for the sample V60A is depicted in Fig. 1. All results are summarized in Table 1. The weight-average molecular masses (M_w), obtained for the unactivated samples, are many times higher than those calculated from the corresponding cuoxam DPs. It is well-known that cellulose is molecularly dispersed in cuoxam at sufficiently low concentrations [18]. Single cellulose molecules could not be detected in NMMNO·MH. This indicates that aggregation of cellulose chains occurs in NMMNO·MH. The apparent aggregation number (n_w), which is calculated from $n_w = M_w/162DP_{cuoxam}$, was 665 for H201 and 635 for V60. Furthermore, the radii of gyration (R_g) of these particles are 188 nm and 204 nm, respectively. The second viral coefficient (A_2) was found to be of the order of 10^{-6} mol cm^3 g^{-2}. This magnitude is typical for systems containing polymeric aggregates or associates [19]. Bochek et al. [20] previously reported on cellulose aggregation in NMMNO·MH blended with dimethylformamide in the mass ratio 50:50.

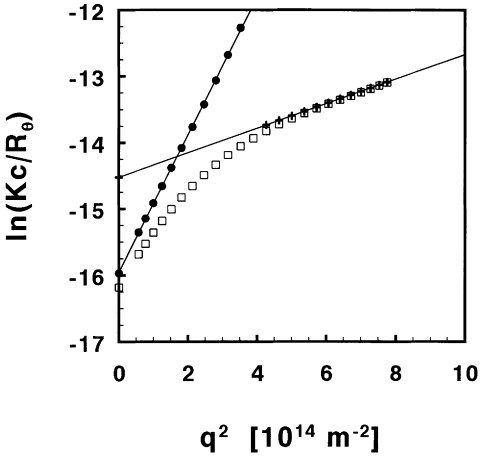

Fig. 2. Guinier factorization of (□) the scattering curve $\ln(Kc/R_\theta)_{q,\,c=0}$ of sample V60A: (+) scattering function of small particles; (●) scattering function of large particles.

In further experiments, we exposed the cellulose samples prior to dissolution to different activation procedures. Only swelling in water has a clear influence on the masses of the particles. M_w or n_w decreased by a factor of about two in the case of the cotton linters and by about three for the wood pulp. The effect of water on the wood pulp was found to be more pronounced than for the cotton linters. Water swells preferably intercrystalline regions of the cellulose and wood pulp has a more heteregeneous supermolecular structure [9].

A marked decrease in the molar mass of the cellulose particles resulted if the cellulose was pretreated with intracrystalline swelling media, concentrated sodium hydroxide solution or liquid ammonia. The radius of gyration, as an indication of the apparent size of the cellulose particles, decreased only slightly after activation of V60 and remained almost unchanged for H201. Assuming that the cellulose particles have a spherical shape, one may estimate the average density of the particles as follows:

$$D = \frac{3M_w}{4\pi R_g^2 N_A} \tag{3}$$

where N_A is Avogadro's constant. The results of this rough approximation are shown in Table 1. For both sample series, the density of the cellulose aggregates decreases with increasing swelling power of the medium used for activation. In other words, if the dissolution process is assumed to occur through the steadily increasing swelling of cellulose, followed by decomposition into single cellulose chains, it can be assumed that in the system cellulose/NMMNO·MH the dissolution freezes at a state of strong swelling. Activation of cellulose led to more swollen particles consisting of fewer molecules.

In Fig. 1 the scattering curves at constant concentrations show a non-linear angular dependence. This bend could be caused by two different effects: (1) the cellulose sample has a very broad molecular mass distribution (MMD) or is even

Table 2
Results of the Guinier factorization

Sample	$w_l M_{wl}$ (g mol^{-1})	R_{gl} (nm)	$w_s M_{ws}$ (g mol^{-1})	R_{gs} (nm)
H201	16.7×10^6	194	2.4×10^6	75
H201W	8.2×10^6	202	1.3×10^6	71
H201S	4.6×10^6	195	0.8×10^6	66
V60	60.1×10^6	232	8.0×10^6	72
V60W	14.4×10^6	191	3.7×10^6	75
V60A	8.6×10^6	175	2.0×10^6	74

bimodal; or (2) at least two species of cellulose particles of different size exist in the solution. SEC/MALLS measurements gave no clear evidence for a bimodal or broad MMD of the H201 and V60 samples. This would indicate that particles with differing sizes exist.

Extrapolation of the measured values to a concentration of zero reveals that the overall scattering curve can be seen as the superposition of two or more scattering functions, which is associated with particles of differing sizes. Therefore, we carried out a Guinier factorization assuming that two dominant sizes of the aggregates exist. This is described in Appendix B and shown in Fig. 2. M_w cannot be estimated absolutely by this method. The calculated molecular masses are weighted with a factor w_i, which gives the fraction of the corresponding particle size. (In what follows, l and s indicate large and small particles, respectively.) The fractions w_i will be estimated by means of other methods in our future work.

Table 2 shows the results of the Guinier factorization. To a rough approximation, the weighted molar masses of the large particles, $w_l M_{wl}$, are of the same magnitude as the overall molecular masses given in Table 1. Futhermore, they are apparently four to eight times greater than the weighted molar masses of the small particles, $w_s M_{ws}$. Note that, in reality, the difference could be far greater as we assume $w_l < w_s$. With respect to the influence of cellulose activation, the values of $w_l M_{wl}$ and $w_s M_{ws}$ show the same behaviour as described above for the general samples. This applies also for the radii of gyration of the larger particles (R_{gl}). However, the radii of gyration of the smaller particles (R_{gs}) of all samples, except for H201S, do not differ significantly. The size of the small particles is nearly independent of both the activation procedure and the source of cellulose.

However, we would like to point out that for increasing values of qR_g the range of structure dimension that is susceptible to light scattering decreases. Therefore, at high scattering angles, parts of large particles as well as real existing small particles are detected as small components. A distinction between them is impossible.

Summarizing, in this study the solution state of cellulose dissolved in NMMNO·MH has been examined. Emphasis was placed on the influence of different methods of cellulose activation. Static light-scattering measurements have been analysed by Guinier's method. Molecular masses of the order of several million g mol^{-1} were observed and the radii of gyration exceeded 160 nm. The second virial coefficient was found to be positive and close to zero. These results suggest that cellulose aggregates exist in solution and that they comprise several hundred cellulose chains. Moreover, the light-scattering curves reflect a bimodal distribution of the particulate phase, consisting of both large and small aggregates. Presumably, the particles observed originate from incompletely disintegrated cellulose crystallites. Activation of cellulose prior to dissolution leads to more swollen particles consisting of significantly fewer cellulose molecules. This effect is more pronounced if intercrystalline swelling media are used, e.g., concentrated sodium hydroxide solution or liquid ammonia. However, the shape and size of the aggregates, especially of the small particles, do not change considerably [21]. A detailed analysis of the geometric shape of cellulose aggregates in NMMNO·MH is planned for publication.

Acknowledgements

We thank the Fonds der Chemischen Industrie (Germany) for financial support. This work was also supported by a grant (T.R.) from the Freistaat Sachsen. The sample V60A was kindly provided by Rhône-Poulenc Rhodia AG, Freiburg. We are indepted to Professors K.-F. Arndt and W. Burchard for stimulating and helpful discussions as well as their comprehensive support of this work. We thank P. Rappold (Lenzing AG) for carrying out SEC measurements.

Appendix A

For a dilute polymer solution, the well-known equation for static laser-light scattering reads:

$$\frac{Kc}{R_\theta} = \frac{1}{M_w P_q} + 2A_2 c + \ldots \quad \text{(A1)}$$

where R_θ is the difference between the Rayleigh ratios of the polymer solution and the solvent at scattering angle θ, c is the polymer mass concentration, and $K = \pi n_0^2 (\delta n/\delta c)^2 / N_A \lambda_0^4$ is the optical constant for the vertically polarized incident light beam; n_0, λ_0, $\delta n/\delta c$ and N_A are the solvent refractive index, the wavelength of light in vacuum, the specific refractive index increment of the polymer solution and Avogadro's constant, respectively; A_2 is the second virial coefficient and M_w is the weight-average molecular mass of the polymer. In Eq. (A1) the terms of higher virial coefficients were neglected. For $q \ll 1$ the scattering factor P_q may be expanded to a good approximation in terms of the scattering vector $q = (4\pi n_0/\lambda_0) \sin(\theta/2)$ as

$$P_q^{-1} = 1 + \tfrac{1}{3} q^2 R_g^2 \quad \text{(A2)}$$

where R_g is the radius of gyration. Eq. (A3) is obtained

through inserting Eq. (A2) into Eq. (A1):

$$\frac{Kc}{R_\theta} = \frac{1}{M_w}\left(1 + \tfrac{1}{3}q^2R_g^2\right) + 2A_2c \quad \text{(A3)}$$

The evaluation of the light-scattering measurements in accordance with Eq. (A3) required two extrapolations, for an interaction-free condition ($c \rightarrow 0$) as well as an interference-free condition ($q \rightarrow 0$). In order to do this, Guiniers's method should be used [22] if the polymer solution contains (1) globular structures, (2) molecules with very high molecular mass (several million g mol^{-1}) and (3) particles of at least two different sizes.

Guinier and Fournet [23] showed that the scattering factor of globular structures can be approximated over a wide range of q^2 by:

$$P_q^{-1} = \exp\left(\tfrac{1}{3}q^2R_g^2\right) \quad \text{(A4)}$$

Wesslau [24] proposed the Guinier–Zimm plot in which $\ln(Kc/R_\theta)$ is plotted against $(q^2 + kc)$, where k is an arbitrary constant. From the intercept and slope of the extrapolation curve $\ln(Kc/R_\theta)_{c,\ q=0}$, the weight-average molecular mass and the second virial coefficient, respectively, can be estimated. The radius of gyration can be obtained from the initial slope of the extrapolation curve $\ln(Kc/R_\theta)_{q,\ c=0}$.

Appendix B

The light scattering of large particles is high at low angles and, vice versa, at high angles the scattering curve asymptotically approaches the scattering function of the small particles. This behaviour can be used to obtain a Guinier factorization of the measured scattering curve into partial scattering functions corresponding to particles with different size. This method was described, for example, by Gruber and Schurz [25].

In this work, the partial scattering function of small aggregates was approximated by making a tangent for $\theta > 90°$ on the $c \rightarrow 0$ extrapolated overall scattering curve, $\ln(Kc/R_\theta)_{q,\ c=0}$. The calculated scattering function was subtracted from the overall curve. The remaining scattering curve was found to be a straight line, which represents the large particles. The slopes of the tangent and the straight line give the radii of gyration of small and large aggregates, respectively. The intercepts give the products of the molecular mass and the concentration of the particles concerned.

References

[1] Johnson DL (Eastman Kodak Co). GB Patent 1 144 048, 1969.
[2] Franks NE, Varga JK (Akzona Inc). US Patent 4 145 532, 1979.
[3] Gagnaire D, Mancier D, Vincendon M. J Polym Sci, Polym Chem Edn 1980;18:13.
[4] McCorsley CC (Akzona Inc). US Patent 4 416 698, 1983.
[5] Berger W. Chemiefasern/Textilind 1994;44/96:747.
[6] Wachsmann U, Diamantoglou M. Das Papier (Darmstadt) 1997;51:660.
[7] Anon. Melliand Textilber 1996;77:98.
[8] Lenz J, Schurz J, Wrentschur E. Acta Polym 1992;43:307.
[9] Krässig HA. In: Huglin MB, editor. Cellulose — structure, accessibility and reactivity. Yverdon: Gordon Breach Science Publishers, 1993.
[10] Turbak AF, El-Kafrawy A, Snyder FW, Auerbach AB (ITT Corp). US Patent 4 302 252, 1981.
[11] Schleicher H, Loth F, Lukanoff B. Acta Polym 1989;40:170.
[12] Burchard W. Trends Polym Sci 1993;1:192.
[13] Morgenstern B, Kammer H-W. Polymer 1999;40:1299.
[14] Kočevar F, Pogačnik M, Povoden V. Das Papier (Darmstadt) 1957;11:301.
[15] Bredereck K, Karstens T, Lentz H, Steinmeier H (Rhône Poulenc Rhodia AG). DE Patent 4 329 937, 1994.
[16] Buijtenhuijs FA, Abbas M, Witteveen AJ. Das Papier (Darmstadt) 1986;40:615.
[17] Seger B. Doctoral thesis. Freiburg: Albert-Ludwigs-Univerität, 1996.
[18] Seger B, Burchard W. Macromol Symp 1994;83:291.
[19] Burchard W. Manuscript in preparation.
[20] Bochek AM, Petropavlovsky GA, Kallistov OV. Cellulose Chem Technol 1993;27:137.
[21] Röder T. Doctoral thesis. Dresden: Technische Universität, 1998.
[22] Burchard W. Adv Polym Sci 1983;48:1.
[23] Guinier A, Fournet G. Small-angle scattering of X-rays. London: Wiley, 1955.
[24] Wesslau H. Makromol Chem 1963;69:213.
[25] Gruber E, Schurz J. Angew Makromol Chem 1973;29/30:121.